Influence of glottal cross-section shape on phonation onset

Annemie Van Hirtum,[a] Bo Wu, and Xavier Pelorson
GIPSA-Lab, UMR CNRS 5216, Grenoble University, F-38031 Grenoble Cedex 1, France

Jorge Lucero
Department of Computer Science, University of Brasilia, Brasilia DF 70910-900, Brazil

(Received 3 February 2014; revised 24 June 2014; accepted 1 July 2014)

Phonation models commonly rely on the assumption of a two-dimensional glottal geometry to assess kinetic and viscous flow losses. In this paper, the glottal cross-section shape is taken into account in the flow model in order to capture its influence on vocal folds oscillation. For the assessed cross-section shapes (rectangular, elliptical, or circular segment) the minimum pressure threshold enabling to sustain vocal folds oscillation is altered for constriction degrees smaller than 75%. The discrepancy between cross-section shapes increases as the constriction degree decreases.
 [http://dx.doi.org/10.1121/1.4889978]

PACS number(s): 43.70.Bk [ZZ] Pages: 853–858

I. INTRODUCTION

Estimation of the pressure distribution within the glottis is an essential part of theoretical phonation modeling aiming to describe vocal fold auto-oscillation characterizing voiced speech production. Flow models applied in theoretical phonation models[1–8] commonly rely on a non-dimensional analysis of the Navier-Stokes equations based on typical values of physiological, geometrical, and flow characteristics of normal voiced speech production by an adult male speaker.[9] From these observations relevant non-dimensional numbers allow one to assume the flow within the glottis during phonation to be incompressible (Mach number, $\mathrm{Ma}^2 \ll 0.1$), laminar inviscid [Reynolds number, $\mathrm{Re} \approx O(10^3)$], quasi-steady (Strouhal number, $\mathrm{Sr} \ll 1$), and two-dimensional (channel aspect ratio or width-to-height ratio, $\mathrm{Ar} \geqslant 4$).[4,5,9–15] The assumption of a two-dimensional glottal flow implies a rectangular glottal cross-section shape for which the height (along the medial-lateral direction) varies along the flow direction $h(x)$ whereas the glottal width (along the anterior-posterior direction) w is fixed.[1–8,16–18] Theoretical flow models based on these assumptions result in a quasi-one-dimensional flow description when accounting for kinetic losses as well as viscous losses.[13,15] Phonation models using such simplified quasi-one-dimensional flow models allow one to express key phonation characteristics, such as the minimum pressure *Pon* required to sustain vocal fold auto-oscillation or phonation, as a function of a limited number of physiological and physically meaningful parameters.[1–8,16,18] Nevertheless, visualization of the auto-oscillation of deformable glottal replicas[19] as well as observations of the glottal geometry during human phonation[9,20,21] revealed that the cross-section shape perpendicular to the main flow direction defers from a rectangular shape. Since the cross-section shape is known to affect boundary layer development, varying the cross-section shape might alter the viscous contribution to the pressure drop. The assumption of a quasi-one-dimensional or two dimensional flow model neglecting the cross-section shape can thus be questioned for normal as well as pathological geometrical conditions. Recently,[22] a flow model was formulated which accounts for kinetic losses as well as the impact of the cross-section shape on viscous losses. It was shown that varying the cross-section shape alters the pressure distribution within a glottal constriction significantly, 20% up to 100% when comparing to the quasi-one-dimensional flow solution.[23] This amounts to the same order of magnitude as well-studied flow events such as the position of flow separation.[14,15,24] Therefore, applying a flow model for which the viscous contribution depends on the cross-section shape potentially affects the outcome of physical or mathematical models of phonation such as the phonation onset pressure threshold *Pon*. The aim of this work is to assess the potential impact of a flow model, which takes into account the cross-section shape, on the outcome of a physical phonation model in comparison with a quasi-one-dimensional flow model. We focus on cross-section shapes relevant for the glottal constriction: rectangular (re), elliptical (el), and circular segment (cs) as illustrated in Fig. 1. In order to provide a fair comparison with the quasi-one-dimensional model approach width w is fixed regardless of the cross-section shape to $w = 20\,\mathrm{mm}$, which is within the range observed on human speakers (15 up to 25 mm[9,15]) and mechanical glottal replicas (20 up to 25 mm[8,25]). All cross-

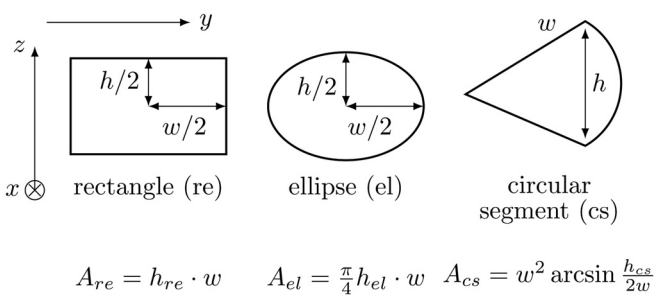

FIG. 1. Cross-section shapes in the (y, z) plane (perpendicular to the main flow direction x) defined by two geometrical parameters—width w and height h, with $\cdot = re, el, cs$—from which geometrical quantities, such as area A, can be derived.

[a]Author to whom correspondence should be addressed. Electronic mail: annemie.vanhirtum@grenoble-inp.fr

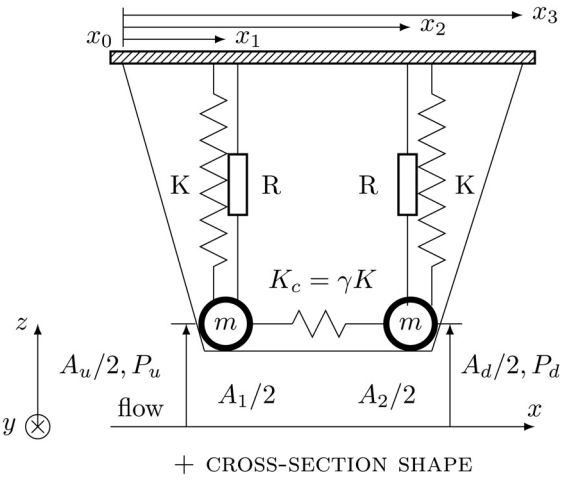

FIG. 2. Schematic representation of a deformable vocal fold structure modeled as a symmetrical reduced two mass model (Ref. 25). The cross-section shape is added to the set of input parameters.

section shapes illustrated in Fig. 1 are fully defined by two geometrical parameters, such as width w and height h, from which the area can be derived.

II. PHONATION ONSET MODELING

A symmetrical two-mass model is used to represent the vocal folds during phonation. Each of the vocal folds is modeled as a reduced spring-mass-damper system with 2 degrees of freedom driven by the pressure difference, $\Delta P = P_u - P_d$, across the masses as illustrated in Fig. 2,[25] where subscripts u and d refer to upstream (u) and downstream (d) of the glottis, respectively. The applied models for glottal airflow, vocal folds mechanics, and acoustic interaction with a downstream and upstream pipe, representing the trachea upstream from the glottis and the vocal tract downstream from the glottis, are severe simplifications of the fluid-structure interaction in the larynx during human voiced sound production.

Based on a non-dimensional analysis of the governing Navier-Stokes equations and typical values of geometrical and flow characteristics for normal phonation by a male adult, the pressure driven flow is described using assumptions of steady, laminar, and incompressible flow through a channel with varying streamwise area $A(x,t)$ for a given cross-section shape.

The streamwise momentum equation of the governing Navier-Stokes equation is further simplified using volume flow conservation $d\Phi/dx = 0$, as[22]

$$-\frac{\Phi^2}{A^3}\frac{dA}{dx} = -\frac{1}{\rho}\frac{dP}{dx} + \nu\left(\frac{\partial^2 U}{\partial y^2} + \frac{\partial^2 U}{\partial z^2}\right), \tag{1}$$

with driving pressure gradient dP/dx, local velocity $U(x,y,z)$, volume flow rate Φ, air density $\rho = 1.2\,\mathrm{kg/m^3}$, and kinematic viscosity of air $\nu = 1.5 \times 10^{-5}\ \mathrm{m^2/s}$. Flow model (1) accounts for kinetic as well as viscous losses and depends therefore on the area as well as on the cross-section shape. Depending on driving pressure, cross-section shape, and area, viscous boundary layer development affects flow development. Consequently, a three-dimensional aspect is added to the model, which is lacking in classically applied flow models. Neglecting the anterior-posterior y-dimension results in the common quasi-one-dimensional flow model (labeled BP) which assumes a fixed glottal width w and streamwise-varying glottal height $h(x,t)$ so that $A_{BP}(x,t) = w \times h(x,t)$. Flow separation along the diverging portion of the glottis is taken into account as $A_s(t) = 1.2 \times \min(A(x,t))$ defining the position of flow separation x_s with $x_1 < x_s \le x_3$. The pressure distribution $P(x,t)$ for $x_0 \le x \le x_s$ is obtained by integration of (1)[22,23] and results in a quadratic equation of volume flow rate Φ as follows:

$$P(x,t) = P_u - \frac{1}{2}\rho\Phi^2\left(\frac{1}{A^2(x,t)} - \frac{1}{A^2(x_0)}\right) + \mu\Phi\int_{x_0}^{x}\frac{dx}{\beta(x,t)}, \quad \text{if } x_0 \le x < x_s, \tag{2}$$

$$P(x,t) = P_d, \quad \text{if } x \ge x_s, \tag{3}$$

with upstream pressure P_u, downstream pressure P_d, dynamic viscosity of air $\mu = 1.8 \times 10^{-5}\ \mathrm{Pa\,s}$, β is introduced to express the viscous contribution to the pressure drop and depends on the cross-section shape as given in Table I.[23] For each cross section shape, β is obtained from the analytical solution—using separation of variables—of a classical Dirichlet problem representing the reduced streamwise momentum equation describing viscous channel flow.[22] In addition, the volume flow rate Φ is estimated as

TABLE I. β as a function of width w and area A for cross-section shapes depicted in Fig. 1 (see Ref. 23).

Shape	$\beta(w,A)$
Rectangle[a]	$\frac{w^3}{6}\left[\frac{A}{2w} - \frac{96w}{\pi^5}\sum_{n=1,3,\ldots}^{\infty}\frac{\tanh(n\pi A/2w^2)}{n^5}\right]$
Ellipse	$\frac{w^2A^3}{(\pi^2w^4 + 16A^2)}$
Circular segment[a]	$\frac{w^4}{4}\left[\frac{\tan 2A/w^2 - 2A/w^2}{4} - \frac{512A^4}{\pi^5w^8}\sum_{n=1,3,\ldots}^{\infty}\frac{1}{n^2(n+4A/\pi w^2)^2(n-4A/\pi w^2)}\right]$
BP[b]	$\frac{A^3}{12w^2}$

[a]Infinite sum is limited to $n \le 60$.
[b]Quasi-one-dimensional flow model.

$$\Phi = \left[\mu \int_{x_0}^{x} \frac{dx}{\beta(x,t)} + \left\{ \left(\mu \int_{x_0}^{x} \frac{dx}{\beta(x,t)} \right)^2 + 2(P_u - P_d)\rho(1/A_s^2 - 1/A^2(x_0)) \right\}^{1/2} \right] \left[\rho \left(1/A_s^2 - 1/A^2(x_0) \right) \right]^{-1}. \quad (4)$$

The vocal folds mechanics are modeled as a symmetrical low order model in which each vocal fold is represented by two identical masses m. The two mass model describes the movement of the two masses perpendicular to the flow direction. The cross-section shape is given and assumed not to vary within the glottis. The mechanical model is further expressed as a function of fixed width w and varying area $A(x,t)$ using the relationship $A(t) = f(w, h(t))$ given in Fig. 1. The main parameters required in the mechanical model are mass m, spring stiffness K, coupling stiffness $K_c = \gamma K$ between the two masses, damping R and critical glottal area threshold A_{crit} triggering vocal folds collision when $A_c < A_{crit}$, with minimum glottal area $A_c = \min(A_1, A_2)$. Whenever collision is detected, the values of K and R are increased to $K = 4K$ and $R = R + 2\sqrt{Km}$. The two masses have the same mechanical parameters K, R, and m as depicted in Fig. 2. With these notations the mechanical model is written as two coupled equations as follows:

$$\frac{m}{2}\frac{d^2A_1}{dt^2} + \frac{R}{2}\frac{dA_1}{dt} + \frac{K(1+\gamma)}{2}A_1 - \frac{\gamma K}{2}A_2 = F_1(A_1, A_2, P_u, P_d), \quad (5)$$

$$\frac{m}{2}\frac{d^2A_2}{dt^2} + \frac{R}{2}\frac{dA_2}{dt} + \frac{K(1+\gamma)}{2}A_2 - \frac{\gamma K}{2}A_1 = F_2(A_1, A_2, P_u, P_d), \quad (6)$$

with $F_{1,2}$ the force exerted by the fluid on the first and second mass, respectively. The mechanical equations at equilibrium reduces to

$$\frac{K(1+\gamma)}{2}\bar{A}_1 - \frac{\gamma K}{2}\bar{A}_2 = F_1\left(\bar{A}_1, \bar{A}_2, \bar{P}_u, \bar{P}_d = 0\right), \quad (7)$$

$$\frac{K(1+\gamma)}{2}\bar{A}_2 - \frac{\gamma K}{2}\bar{A}_1 = F_2\left(\bar{A}_1, \bar{A}_2, \bar{P}_u, \bar{P}_d = 0\right), \quad (8)$$

from which the equilibrium positions for a given upstream pressure $\bar{P}_u$ are derived by a fixed point method. Assuming a small perturbation (a_1, a_2, p_u, p_d) of the quantities around the equilibrium values $eq = (\bar{A}_1, \bar{A}_2, \bar{P}_u, P_d = 0)$ as

$$A_1 = \bar{A}_1 + a_1, \quad A_2 = \bar{A}_2 + a_2, \quad (9)$$

$$P_u = \bar{P}_u + p_u, \quad P_d = p_d, \quad (10)$$

results in the following set of equations:

$$\frac{m}{2}\frac{d^2a_1}{dt^2} + \frac{R}{2}\frac{da_1}{dt} + \frac{K(1+\gamma)}{2}a_1 - \frac{\gamma K}{2}a_2 = \frac{\partial F_1}{\partial A_1}\bigg|_{eq} a_1 + \frac{\partial F_1}{\partial A_2}\bigg|_{eq} a_2 + \frac{\partial F_1}{\partial P_u}\bigg|_{eq} p_u + \frac{\partial F_1}{\partial P_d}\bigg|_{eq} p_d, \quad (11)$$

$$\frac{m}{2}\frac{d^2a_2}{2} + \frac{R}{2}\frac{da_2}{dt} + \frac{K(1+\gamma)}{2}a_2 - \frac{\gamma K}{2}a_1 = \frac{\partial F_2}{\partial A_1}\bigg|_{eq} a_1 + \frac{\partial F_2}{\partial A_2}\bigg|_{eq} a_2 + \frac{\partial F_2}{\partial P_u}\bigg|_{eq} p_u + \frac{\partial F_2}{\partial P_d}\bigg|_{eq} p_d. \quad (12)$$

Acoustical coupling between the vocal folds and a uniform upstream tube with length L_u representing the trachea and/or a uniform downstream tube with length L_d representing the vocal tract is important when the acoustical resonance frequencies of the pipe and the vocal fold resonance frequencies are close.[25,26] The acoustic set of equations for frequencies up to and around the first vocal tract resonance frequency[5,27] is given as

$$\frac{d^2\psi_d}{d^2t} + \frac{\omega_d}{Q_d}\frac{d\psi_d}{dt} + \omega_d^2\psi_d = \frac{Z_d\omega_d}{Q_d}\phi, \quad (13)$$

$$\frac{d^2\psi_u}{d^2t} + \frac{\omega_u}{Q_d}\frac{d\psi_u}{dt} + \omega_u^2\psi_u = -\frac{Z_u\omega_u}{Q_u}\phi, \quad (14)$$

with $\partial\psi_{u,d}/\partial t = p_{u,d}$ the acoustic pressure and ϕ the unsteady portion of the volume flow velocity, $w_{u,d}$ the acoustical pipe resonance frequencies, $Q_{u,d}$ the quality factor and $Z_{u,d}$ the peak value of the acoustical impedance. As for the mechanical equations assuming small variations around equilibrium results in

$$\frac{d^2\psi_d}{d^2t} + \frac{\omega_d}{Q_d}\frac{d\psi_d}{dt} + \omega_d^2\psi_d = \frac{Z_d\omega_d}{Q_d}\left(\frac{\partial\Phi}{\partial A_1}\bigg|_{eq} a_1 + \frac{\partial\Phi}{\partial A_2}\bigg|_{eq} a_2 + \frac{\partial\Phi}{\partial P_u}\bigg|_{eq} p_u + \frac{\partial\Phi}{\partial P_d}\bigg|_{eq} p_d\right), \quad (15)$$

$$\frac{d^2\psi_u}{d^2t} + \frac{\omega_u}{Q_d}\frac{d\psi_u}{dt} + \omega_u^2\psi_u = -\frac{Z_u\omega_u}{Q_u}\left(\frac{\partial\Phi}{\partial A_1}\bigg|_{eq} a_1 + \frac{\partial\Phi}{\partial A_2}\bigg|_{eq} a_2 + \frac{\partial\Phi}{\partial P_u}\bigg|_{eq} p_u + \frac{\partial\Phi}{\partial P_d}\bigg|_{eq} p_d\right). \quad (16)$$

Consequently, assuming small variations around equilibrium results in a coupled set of equations obtained from (11), (12), (15), and (16). The system can be expressed in state-space form as

$$\dot{X} = MX \quad (17)$$

with $X = [a_1, a_2, \psi_u, \psi_d, da_1/dt, da_2/dt, d\psi_u/dt, d\psi_d/dt]$ and

$$M = \left[\begin{array}{c|c} A & B \\ \hline C & D \end{array}\right]$$

with null matrix $A = \not{4}_{4,4}$, identity matrix $B = I_4$ and matrices C and D defined as

$$C = \begin{bmatrix} -\frac{K(1+\gamma) - 2\frac{\partial F_1}{dA_1}\big|_{eq}}{m} & \frac{\gamma K + 2\frac{\partial F_1}{dA_2}\big|_{eq}}{m} & 0 & 0 \\ \frac{\gamma K + 2\frac{\partial F_2}{dA_1}\big|_{eq}}{m} & -\frac{K(1+\gamma) - 2\frac{\partial F_2}{dA_2}\big|_{eq}}{m} & 0 & 0 \\ \frac{Z_d\omega_d}{Q_d}\frac{\partial \Phi}{\partial A_1}\big|_{eq} & \frac{Z_d\omega_d}{Q_d}\frac{\partial \Phi}{\partial A_2}\big|_{eq} & 0 & -\omega_d^2 \\ -\frac{Z_u\omega_u}{Q_u}\frac{\partial \Phi}{\partial A_1}\big|_{eq} & -\frac{Z_u\omega_u}{Qu}\frac{\partial \Phi}{\partial A_2}\big|_{eq} & -\omega_u^2 & 0 \end{bmatrix} \tag{18}$$

and

$$D = \begin{bmatrix} -\frac{R}{m} & 0 & \frac{2}{m}\frac{\partial F_1}{\partial P_u}\big|_{eq} & \frac{2}{m}\frac{\partial F_1}{\partial P_d}\big|_{eq} \\ 0 & -\frac{R}{m} & \frac{2}{m}\frac{\partial F_2}{\partial P_u}\big|_{eq} & \frac{2}{m}\frac{\partial F_2}{\partial P_d}\big|_{eq} \\ 0 & 0 & \frac{Z_d\omega_d}{Q_d}\frac{\partial \Phi}{\partial P_u}\big|_{eq} & -\frac{\omega_d}{Q_d} + \frac{Z_d\omega_d}{Q_d}\frac{\partial \Phi}{\partial P_d}\big|_{eq} \\ 0 & 0 & -\frac{\omega_u}{Q_d} - \frac{Z_u\omega_u}{Q_u}\frac{\partial \Phi}{\partial P_u}\big|_{eq} & -\frac{Z_u\omega_u}{Q_u}\frac{\partial \Phi}{\partial P_d}\big|_{eq} \end{bmatrix}. \tag{19}$$

The system will become instable, corresponding to the onset of auto-oscillation, when the real portion of an eigenvalue of M is positive.

III. PHONATION ONSET THRESHOLD PRESSURE

We search the influence of the cross-section shapes, depicted in Fig. 1, on the predicted auto-oscillation onset by assessing the onset pressure Pon. Therefore, a linear stability analysis is performed by considering the real portion of the eigenvalues of M for increasing upstream pressure P_u for different cross-section shapes and for different initial constriction degrees $1 - A^0/A_u$, with superscript 0 denoting the minimum channel value in absence of flow and subscript u indicating the value upstream from the glottis. Concretely, the constriction degree is varied from 50% up to 90% whereas the width w is fixed. The resulting aspect ratios $Ar^0 = w/h^0$ yield $1 < Ar^0 < 9$ and depend on the cross-section shape as illustrated in Fig. 3(a). For fixed width w the aspect ratios of the quasi-one dimensional geometry and the rectangular cross-section shape match since $A^0 = w \times h^0_{re}$ holds in both cases. The corresponding hydraulic diameter of the constriction is the same for the rectangular cross section shape and circular segment whereas the discrepancy for the elliptical shape is smaller than 16% for all constriction degrees.

Besides the constriction degree and the cross-section shape the other model parameters are taken constant with values taken from Ref. 25 and correspond to a configuration for which auto-oscillation was experimentally observed. Concretely, the following values are used: Geometry $[x_0\, x_1\, x_2\, x_3] = [0\ 1\ 4\ 5]$mm, width $w = 20$ mm, upstream area $A_{u,d} = 400\,\text{mm}^2$, masses $m = 0.2$ g, spring stiffness $K = 131\,\text{N m}^{-2}$, coupling spring stiffness $K_c = 65\,\text{N m}^{-2}$, damping $R = 0.006\,\text{N s m}^{-2}$ and collision threshold $A_{crit} = 0.4\,\text{mm}^2$, upstream pipe lengths $L_u = 0$ cm and downstream pipe length $L_d = 17$ cm, acoustic pipe resonance frequencies $\omega_u = 0$ and $\omega_d = 2965$ rad/s, quality factors $Q_u = 0$ and $Q_d = 51$, and acoustic impedance peaks $Z_u = 0$ and $Z_d = 54\,\text{MPa s m}^{-3}$). Simulation results for phonation onset pressure P_{on} are illustrated in Fig. 3(b) as a function of constriction degree $1 - A^0/A_u$ and in Fig. 3(c) as a function of aspect ratio $Ar^0 = w/h^0$.

IV. DISCUSSION AND CONCLUSION

For large constriction degrees [greater than 75% in Fig. 3(b)] the cross-section shape can be neglected. For medium or small constriction degrees [smaller than 75% in Fig. 3(b)] the predicted phonation onset threshold pressure Pon depends on the cross-section shape since less pressure is required to sustain oscillation for a circular segment cross-section shape than for a rectangular or elliptical cross-section shape. The discrepancy between Pon estimations belonging to different cross-section shapes increases as the constriction degree [Fig. 3(b)] or aspect ratio [Fig. 3(c)] decreases. Moreover, it is observed that for the assessed range of constriction degrees and associated aspect ratios [from 2 up to 9 illustrated in Fig. 3(a)], a rectangular geometry can be modeled using a quasi-one-dimensional (BP) flow approximation. The simulated phonation onset threshold

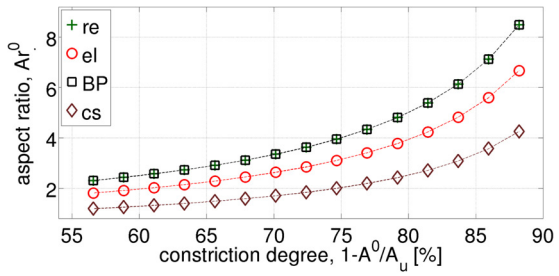

(a) $Ar^0_\cdot(1 - A^0/A_u)$ for $\cdot$ =re,el,BP,cs

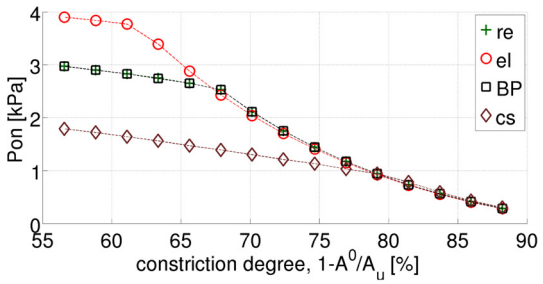

(b) $Pon(1 - A^0/A_u)$ for $\cdot$ =re,el,BP,cs

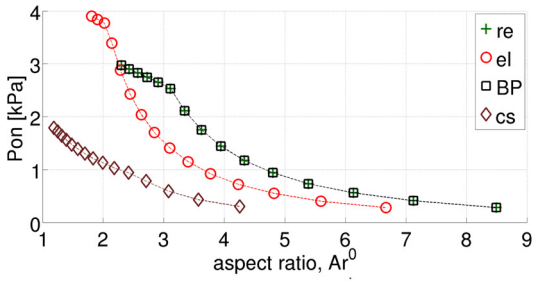

(c) $Pon(Ar^0_\cdot)$ for $\cdot$ =re,el,BP,cs

FIG. 3. (Color online) (a) Aspect ratio $Ar^0_\cdot = w/h^0_\cdot$ as a function of initial constriction degree $1 - A^0/A_u$ for cross-section shapes (rectangle—re; ellipse—el; quasi-one-dimensional—BP; and circular segment—cs) with fixed width $w = 20$ mm. (b) Modeled onset pressure threshold *Pon* as a function of constriction degree $1 - A^0/A_u$, and (c) modled onset pressure *Pon* as a function of aspect ratio $Ar^0_\cdot$.

pressures *Pon* suggest that for large constriction degrees [greater than 75% in Fig. 3(b)] the model outcome depends on an accurate value of the constricted area A^0 as a model input parameter. For medium or smaller constriction degrees [smaller than 75% in Fig. 3(b)], it is necessary to quantify the constricted area A^0 as well as to obtain information on the cross-section shape in order to capture the impact of the cross-section shape on the viscous losses in the flow model. When the aspect ratio Ar^0 is used as model input parameter [Fig. 3(c)] additional information on the cross-section shape is required as a model input parameter for all aspect ratios. Since the normal range of the constriction ratio and aspect ratio for human phonation yield $55 \le 1 - A^0/A_u \le 80\%$ and $2 \le Ar^0_\cdot \le 7$, respectively,[4,5,9–15] current results show the relevance to account for the cross-section shape when modeling human phonation. The current model findings with respect to the impact of the cross-section shape on phonation onset need yet to be validated experimentally. In addition, given the severe influence of the cross-section shape on the predicted phonation onset pressure *Pon*, it is of interest to extent the current model approach to an arbitrary cross-section shape. This seems important in order to enlarge the relevance of simplified physical phonation models for applications such as vocal folds pathologies affecting the cross-section shape of the glottis during phonation. Finally, a detailed model analysis and parameter sensitivity study is motivated for future studies.

[1]K. Ishizaka and J. Flanagan, "Synthesis of voiced sounds from a two-mass model of the vocal cords," Bell Syst. Tech. J. **51**, 1233–1267 (1972).
[2]I. Titze, "The physics of small-amplitude oscillation of the vocal folds," J. Acoust. Soc. Am. **83**, 1536–1552 (1988).
[3]J. Awrejcewicz, "Dynamics of the human vocal cords," J. Theoretical Appl. Mech. **29**, 557–577 (1991).
[4]X. Pelorson, A. Hirschberg, R. Van Hasselt, A. Wijnands, and Y. Auregan, "Theoretical and experimental study of quasisteady-flow separation within the glottis during phonation. application to a modified two-mass model," J. Acoust. Soc. Am. **96**, 3416–3431 (1994).
[5]N. Lous, G. Hofmans, N. Veldhuis, and A. Hirschberg, "A symmetrical two-mass vocal-fold model coupled to vocal tract and trachea, with application to prosthesis design," Acta Acust. **84**, 1135–1150 (1998).
[6]J. Lucero, "The minimum lung pressure to sustain vocal fold oscillation," J. Acoust. Soc. Am. **98**, 779–784 (1995).
[7]B. Story and I. Titze, "Voice simulation with a body-cover model of the vocal folds," J. Acoust. Soc. Am. **97**, 1249–1260 (1995).
[8]N. Ruty, X. Pelorson, A. Van Hirtum, I. Lopez, and A. Hirschberg, "An in-vitro setup to test the relevance and the accuracy of low-order vocal folds models," J. Acoust. Soc. Am. **121**, 479–490 (2007).
[9]R. Daniloff, G. Schuckers, and L. Feth, *The Physiology of Speech and Hearing* (Prentice Hall, Englewood Cliffs, NJ, 1980), 453 pp.
[10]E. Holmberg, R. Hillman, and J. Perkell, "Glottal airflow and transglottal air pressure measurements for male and female speakers in soft, normal and loud voice," J. Acoust. Soc. Am. **84**, 511–529 (1988).
[11]K. Stevens, *Acoustic Phonetics* (MIT Press, MA, 1998), 606 pp.
[12]L. Koenig, W. Menci, and J. Lucero, "Multidimensional analyses of voicing offsets and onsets in female speakers," J. Acoust. Soc. Am. **118**, 2535–2550 (2005).
[13]J. Cisonni, A. Van Hirtum, X. Pelorson, and J. Willems, "Theoretical simulation and experimental validation of inverse quasi one-dimensional steady and unsteady glottal flow models," J. Acoust. Soc. Am. **124**, 535–545 (2008).
[14]A. Van Hirtum, J. Cisonni, and X. Pelorson, "On quasi-steady laminar flow separation in the upper airways," Commun. Numer. Meth. Eng. **25**, 447–461 (2009).
[15]J. Cisonni, A. Van Hirtum, X. Luo, and X. Pelorson, "Experimental validation of quasi one-dimensional and two-dimensional steady glottal flow models," Med. Biol. Eng. Comput. **48**, 903–910 (2010).
[16]A. Barney, C. Shadle, and P. Davies, "Fluid flow in a dynamic mechanical model of the vocal folds and tract. I. measurements and theory," J. Acoust. Soc. Am. **105**, 444–455 (1999).
[17]R. Laje, T. Gardner, and G. Mindlin, "Continuous model for vocal fold oscillations to study the effect of feedback," Phys. Rev. E **64**, 1–7 (2001).
[18]J. Lucero, A. Van Hirtum, N. Ruty, J. Cisonni, and X. Pelorson, "Validation of theoretical models of phonation threshold pressure with data from a vocal fold mechanical replica," J. Acoust. Soc. Am. **125**, 632–635 (2009).
[19]A. Van Hirtum, J. Cisonni, N. Ruty, X. Pelorson, I. Lopez, and F. van Uittert, "Experimental validation of some issues in lip and vocal fold physical models," Acta Acust. **93**, 314–323 (2007).
[20]E. Yumoto, Y. Kadota, and T. Mori, "Vocal fold vibration viewed from the tracheal side in living human beings," Otolaryngol. Head Neck Surgery **115**, 329–334 (1996).
[21]M. Doellinger, D. Berry, and G. Berke, "Medial surface dynamics of an in vivo canine vocal fold during phonation," J. Acoust. Soc. Am. **117**, 3174–3183 (2005).
[22]B. Wu, A. Van Hirtum, and X. Luo, "Pressure driven steady flow in constricted channels of different cross section shapes," Int. J. Appl. Mech. **5**, 1–19 (2013).
[23]B. Wu, A. Van Hirtum, X. Pelorson, and X. Luo, "The influence of glottal cross-section shape on theoretical flow models," J. Acoust. Soc. Am. **134**, 909–912 (2013).

[24]P. Sidlof, O. Doare, O. Cadot, and A. Chaigne, "Measurement of flow separation in a human vocal folds model," Exp. Fluids **51**, 123–136 (2011).
[25]J. Cisonni, A. Van Hirtum, X. Pelorson, and J. Lucero, "The influence of geometrical and mechanical input parameters on theoretical models of phonation," Acta Acust. **97**, 291–302 (2011).
[26]J. Lucero, K. Lourenco, N. Hermant, A. Van Hirtum, and X. Pelorson, "Effect of source tract acoustical coupling on the oscillation onset of the vocal folds," J. Acoust. Soc. Am. **132**, 403–411 (2012).
[27]J. Cullen, J. Gilbert, and M. Campbell, "Brass instruments: Linear stability analysis and experiments with an artificial mouth," Acta Acoust. **86**, 704–724 (2000).